ZenoTOF 7600 system

The Zeno revolution is now...

The Zeno trap & electron activated dissociation (EAD) technology – a powerful combination of unparalleled MS/MS sensitivity and a step-change in fragmentation technology.

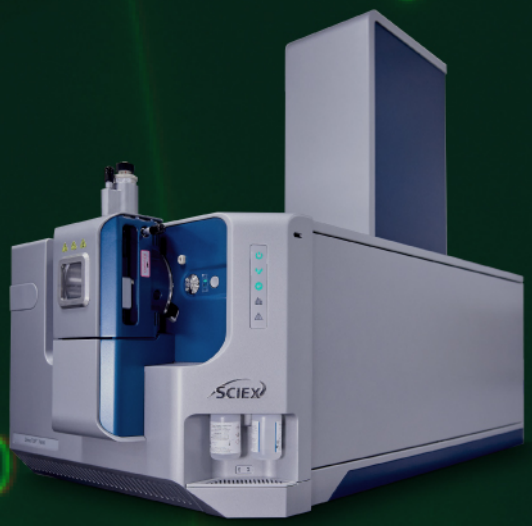

Download 2 exclusive SCIEX white papers:

- Zeno trap: The next era of sensitivity for accurate mass
- Electron activated dissociation (EAD): A step change in fragmentation technology

Download now

SCIEX
The Power of Precision

Received: 7 April 2020 | Revised: 18 May 2020 | Accepted: 19 May 2020

DOI: 10.1002/jms.4578

SPECIAL FEATURE: TUTORIAL

Journal of MASS SPECTROMETRY WILEY

Native mass spectrometry—A valuable tool in structural biology

Marie Barth | Carla Schmidt

Interdisciplinary Research Center HALOmem, Charles Tanford Protein Center, Institute for Biochemistry and Biotechnology, Martin Luther University Halle-Wittenberg, Halle, Germany

Correspondence
Carla Schmidt, Interdisciplinary Research Center HALOmem, Charles Tanford Protein Center, Institute for Biochemistry and Biotechnology, Martin Luther University Halle-Wittenberg, Kurt-Mothes-Str. 3a, 06120 Halle, Germany.
Email: carla.schmidt@biochemtech.uni-halle.de

Funding information
European Regional Development Funds, Grant/Award Number: ZS/2016/04/78115; Federal Ministry for Education and Research, Grant/Award Number: 03Z22HN22

Abstract

Proteins and the complexes they form with their ligands are the players of cellular action. Their function is directly linked with their structure making the structural analysis of protein-ligand complexes essential. Classical techniques of structural biology include X-ray crystallography, nuclear magnetic resonance spectroscopy and recently distinguished cryo-electron microscopy. However, protein-ligand complexes are often dynamic and heterogeneous and consequently challenging for these techniques. Alternative approaches are therefore needed and gained importance during the last decades. One alternative is native mass spectrometry, which is the analysis of intact protein complexes in the gas phase. To achieve this, sample preparation and instrument conditions have to be optimised. Native mass spectrometry then reveals stoichiometry, protein interactions and topology of protein assemblies. Advanced techniques such as ion mobility and high-resolution mass spectrometry further add to the range of applications and deliver information on shape and microheterogeneity of the complexes. In this tutorial, we explain the basics of native mass spectrometry including sample requirements, instrument modifications and interpretation of native mass spectra. We further discuss the developments of native mass spectrometry and provide example spectra and applications.

KEYWORDS
ESI, ion mobility, native MS, protein complexes, protein interactions, protein structure

1 | INTRODUCTION

The development of two soft ionisation techniques, namely, matrix-assisted laser desorption/ionization[1,2] and electrospray ionisation (ESI),[3] in the late 1980s made the analysis of intact biomolecules possible and advanced the field of biomolecular mass spectrometry (MS). In particular, ESI is nowadays indispensable for proteomics, lipidomics, glycomics or, generally speaking, the analysis of various biomolecules in solution. Improvements in instrumentation and technology further advanced the application of MS and enabled the development of numerous specialised techniques. One such technique is 'native' MS, which is the analysis of intact proteins and protein complexes in the gas phase of a mass spectrometer.

During native MS, noncovalent interactions between proteins and their ligands, for example, other proteins, nucleotides, lipids or other small molecules, are maintained.[4,5] The obtained mass spectra therefore reveal the composition and stoichiometry of the formed complexes. Native MS further provides information on subunit interactions and topology as well as heterogeneity of the assemblies. The mass range spans from individual subunits or ligands up to large assemblies giving clues on the stability of the complexes as well as preferred interactions. Native MS, consequently, takes an important

role in the structural analysis of proteins and protein complexes by MS.

However, there are some prerequisites for the application of native MS: Sample preparation often has to be customised, and an optimal instrument environment for transmission of high-mass complexes under nondenaturing conditions has to be achieved. In addition, data analysis is not automated and requires an experienced scientist. In this tutorial, we introduce the application of native MS, including sample preparation, instrument requirements and data analysis, and discuss advanced applications such as ion mobility (IM) and high-resolution native MS.

2 | SAMPLE PREPARATION FOR NATIVE MS

The first step of sample preparation is the purification of the protein or protein complex of interest (Figure 1). This is most commonly achieved by overexpressing the protein or protein complex in bacterial cells followed by purification using affinity tags. Nonetheless, the protein complexes of interest can also be obtained from natural sources such as plant or organ tissue. Each purification protocol has to be optimised individually to obtain sufficient amounts for further analyses. However, during purification, interfering substances, which cause signal suppression during ESI-MS analysis, are commonly used.[6–8] These substances are, for instance, metal cations, inorganic ions, alkylammonium and guanidinium salts or typical buffers such as HEPES, PBS, MES, MOPS or Tris. In addition, some proteins (for instance, membrane proteins) require detergents or stabilizers such as Tween, Chaps, Triton, SDS, PEG, PPG or urea. All these interfering substances need to be removed or at least diluted prior to native MS analysis. Additives, electrolytes and supercharging reagents can counteract effects of nonvolatile buffer components.[9–12] However, this strategy is only applicable for low concentrations of nonvolatile components and might increase frequency of instrument cleaning. The main challenge of sample preparation is therefore to preserve noncovalent interactions and the native structure of the proteins and protein complexes and, at the same time, provide an MS compatible protein solution at sufficient concentration in the range of 1–20 μM. A robust one-step affinity purification protocol was therefore introduced allowing efficient and rapid purification of endogenous protein complexes by coupling affinity purification and buffer exchange.[13]

Nonetheless, for native MS, the purification buffer has to be exchanged to an aqueous and volatile solvent like ammonium acetate, ammonium bicarbonate or ammonium formate prior to analysis. In most cases, ammonium acetate at a pH between 6 and 8 is the solution of choice. The components ammonia and acetic acid are volatile and evaporate readily during ESI.[14] In addition, high concentrations of ammonium acetate reduce interfering effects of nonvolatile buffers such as HEPES or Tris.[6,11,14] However, one has to keep in mind that ammonium acetate does not provide ideal physiological conditions of the protein complexes.[15]

The purification buffer is typically exchanged using miniaturised gel filtration columns, molecular weight cut-off filters or dialysis devices (Figure 1). Automated inline gel filtration maximises storage times of the proteins in a suitable buffer before analysis.[16] However, in some cases, the protein precipitates or aggregates during buffer exchange. Possible solutions are increasing the ionic strength of the buffer (higher ammonium acetate concentrations above the typically used 100–200 mM) or working at a different pH. Filters are used to deplete nonvolatile buffer components like salts and detergents and simultaneously concentrate the sample.[17] However, the proteins might be absorbed at the membrane or detergent micelles are too large to pass through the filter membrane and remain in the solution. Therefore, different membrane materials and pore sizes have to be tested.[17] Note that larger pore sizes might cause loss of individual subunits which might have dissociated from the protein complexes. Dialysis and in particular online microdialysis[18] have the advantage of limited dilution of the protein concentration; however, incomplete removal of nonvolatile buffer components and a more complex technical set-up are disadvantageous. In a nutshell, the buffer, the

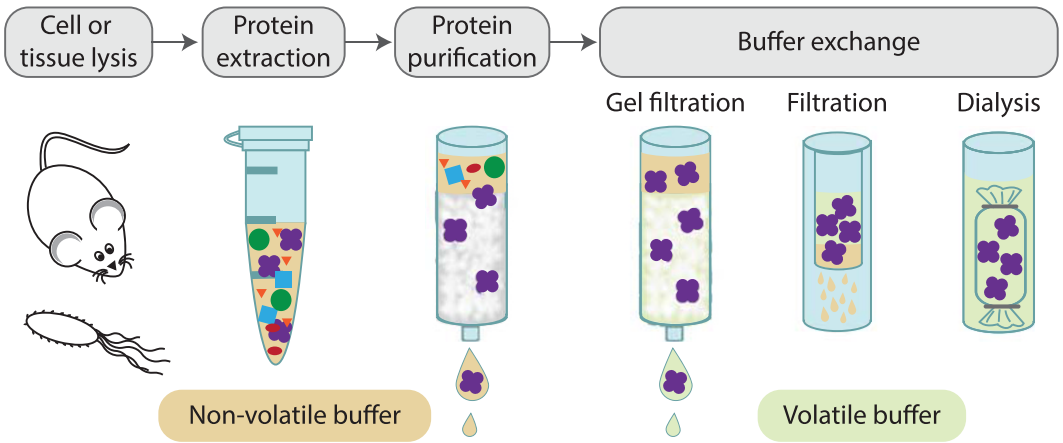

FIGURE 1 Sample preparation for native MS. The protein or protein complex is purified from cell or tissue lysate, usually following traditional purification protocols or affinity purification when the proteins are overexpressed with an affinity tag. The purified protein is stored in purification buffer until MS analysis. Following gel filtration, filtration or dialysis, the buffer is exchanged against an aqueous and volatile solution

exchange method and the concentration have to be carefully selected and optimised for each protein or protein complex.

Recent developments in sample preparation for native MS include the analysis of protein and protein complexes in buffers of physiological ionic strength and containing nonvolatile components. For this, small emitter tips (0.5 μm) are employed leading to a decrease in salt adducts with decreasing tip size.[19] However, pulling emitters with small tip diameters requires specialised expertise. Another recent development includes the analysis of overexpressed proteins directly from cell lysate.[20,21] For this, the cells that overexpress a certain protein are lysed in ammonium acetate and subsequently analysed by native MS. High concentrations of ammonium acetate (typically 1 M) facilitate removal of salt adducts. Further developments include the automated, online buffer exchange of cell lysates.[22]

3 | INSTRUMENT MODIFICATIONS FOR TRANSMISSION OF HIGH-MASS COMPLEXES

To maintain noncovalent interactions of proteins and their ligands during native MS experiments, the employed mass spectrometer is usually modified for transmission of high-mass complexes (Figure 2). Traditionally, quadrupole time-of-flight (Q-ToF) mass spectrometers, composed of a quadrupole mass filter, a hexapole collision-gas cell and a ToF mass analyser,[23] are used for native MS.[24] Major modifications of the Q-ToF mass spectrometer include (i) changes in the pressure gradient in the different pumping stages of the instrument and (ii) reducing the radiofrequency of the quadrupole mass analyser.[24]

i When compared with conventional Q-ToF instruments, the pressure of all pumping stages is increased, and as a consequence, transmission of high *m/z* ions is improved.[24–27] This is mainly achieved by collisional cooling and, at the same time, collisional focusing of high *m/z* ions in the hexapole ion guide of the initial vacuum stage.[25,28,29] In detail, the background pressure in the initial vacuum stages of the mass spectrometer (p1) is raised by reducing the pumping of the rotary pump; for this, the background pressure p1 is controlled through a SpeediValve and, depending on the required mass range, varies between 3 to 7 mbar. Ions that enter the mass spectrometer through the atmospheric pressure ion source lose kinetic energy and axial motion, and the ion beam is confined towards the central axis of the ion guide. At this stage, partly solvated ions are activated by collisions with background gas atoms and subsequently lose residual attached solvent molecules. The energy input for this activation should not induce dissociation of the complexes, and acceleration voltages should therefore be controlled carefully. The pressure of the second pumping stage (p2) is increased and optimised by fitting an additional leak valve allowing a neutral gas such as argon or xenon to admit to this pumping stage resulting in pressures between 3×10^{-4} and 1×10^{-2} mbar. The third pumping stage (p3) holds a pressure of $3–10 \times 10^{-5}$ mbar. The ToF analyser operates at pressures in the upper 10^{-7} mbar range.[24] See Figure 2 for an overview on the pumping stages.

ii Quadrupoles transmit ions to an upper limit that depends on the radiofrequency and amplitude as well as the diameter (or inner radius) between the quadrupole rods. The quadrupole of a conventional Q-ToF mass spectrometer operates at a frequency of 832 kHz resulting in an upper limit of 4190 *m/z*.[23] For native MS, the frequency is usually decreased to 300 kHz allowing transmission of ions up to approximately 32 000 *m/z*.[24]

In addition to the above discussed changes in the pressure gradient and the quadrupole, the aperture of the collision-gas cell entrance and exit is decreased to allow higher collisional pressure; at the same

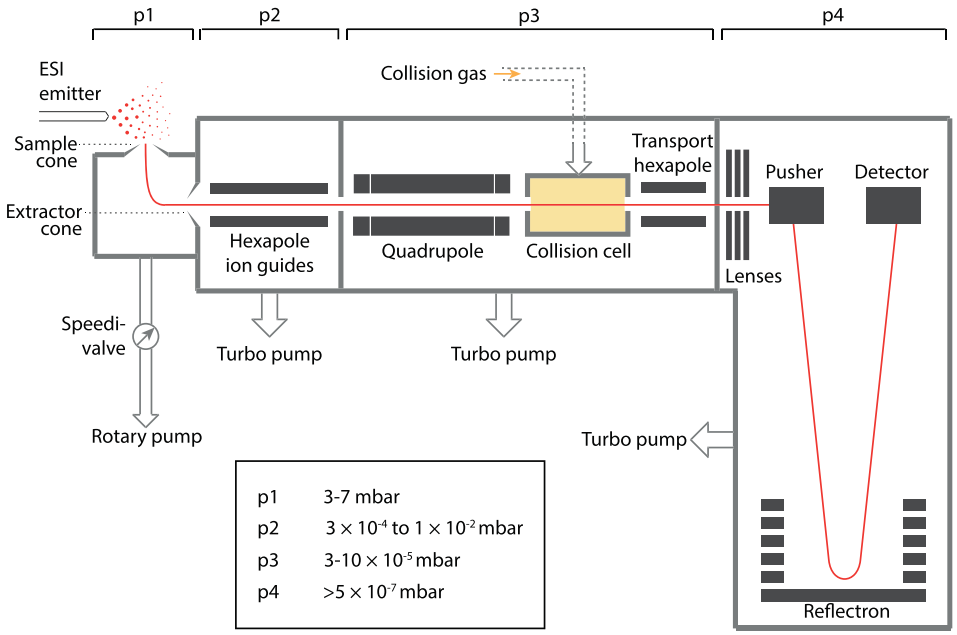

FIGURE 2 Schematic of a modified Q-ToF mass spectrometer. Relevant elements and components are shown. Ions are generated by ESI. The ion beam (red) is shown throughout the instrument. The different pumping stages (p1 to p4) are indicated and typical pressures are given. See Section 3 for details

time, the orifice is optimised for transmission of precursor and product ions obtained in native MS experiments.[24]

4 | TRANSFER OF PROTEINS AND PROTEIN COMPLEXES INTO THE GAS PHASE

For native MS, ions are usually obtained from ESI in positive ion mode. The first step during ESI is the formation of charged droplets from the analyte solution. This is achieved by applying a potential of several kilovolts to the spray emitter (the 'needle') pulling the liquid towards the counter electrode. At a certain voltage, a so-called 'Taylor cone' is formed[30] and a spray of charged droplets is emitted from the tip of the cone (Figure 3A). The introduction of nano-ESI greatly facilitated the analysis of proteins; the smaller size of the droplets enables the use of aqueous solutions, tolerates higher salt concentrations and, importantly, requires lower sample amounts.[31] There are different models that explain the ionisation process of molecules from charged droplets.[32,33] Accordingly, low molecular weight species such as peptides, lipids or sugars are thought to be expelled in a solvation shell from charged droplets when, due to evaporation of the solvent, the droplet charge is sufficiently high. The remaining solvent shell is then lost at the interface of the mass spectrometer ('ion evaporation model').[34] A single large, globular species such as a folded protein usually occupies one charged droplet. After complete evaporation of the solvent, the charge is transferred to the analyte ion ('charged residue model'; Figure 3B).[35] Ions of unfolded proteins, in contrast, are generated through a different mechanism; due to their large hydrophobic proportion, they are unstable in the interior of charged droplets and migrate to the droplet surface. After one chain terminus has been expelled into the gas phase, the remaining chain is then ejected sequentially ('chain ejection model').[36]

Even though noncovalent interactions of protein complexes can be maintained during transfer into the gas phase, one has to keep in mind that the gas phase structure of a protein or protein complex might differ from its solution structure. Possible reasons are, amongst others, the decreasing pH of shrinking ESI droplets,[37] applied heat during ESI[38] and, most importantly, loss of the protein's hydration shell.[39] Accordingly, molecular dynamics simulations revealed collapse of charged side chains and formation of a network of electrostatic interactions on the protein surface when fully desolvated in the gas phase; since the protein's backbone remained unchanged in these simulations, stabilisation of the structure through these newly formed interactions is assumed.[40] In contrast, at long time periods, formation of new conformers as a result of unfolding and refolding in the gas phase was observed experimentally.[41–43] Importantly, these processes strongly depend on the time-scale and experimental conditions.[44] Several computational and experimental studies confirmed that the overall structures with only minimal differences between solution state and gas phase can be maintained in the typical analysis time frame.[40,45–47] In an optimised set-up, the transfer of proteins and protein complexes by ESI while maintaining solution-like structures is therefore possible and allows the analysis of intact assemblies.[44]

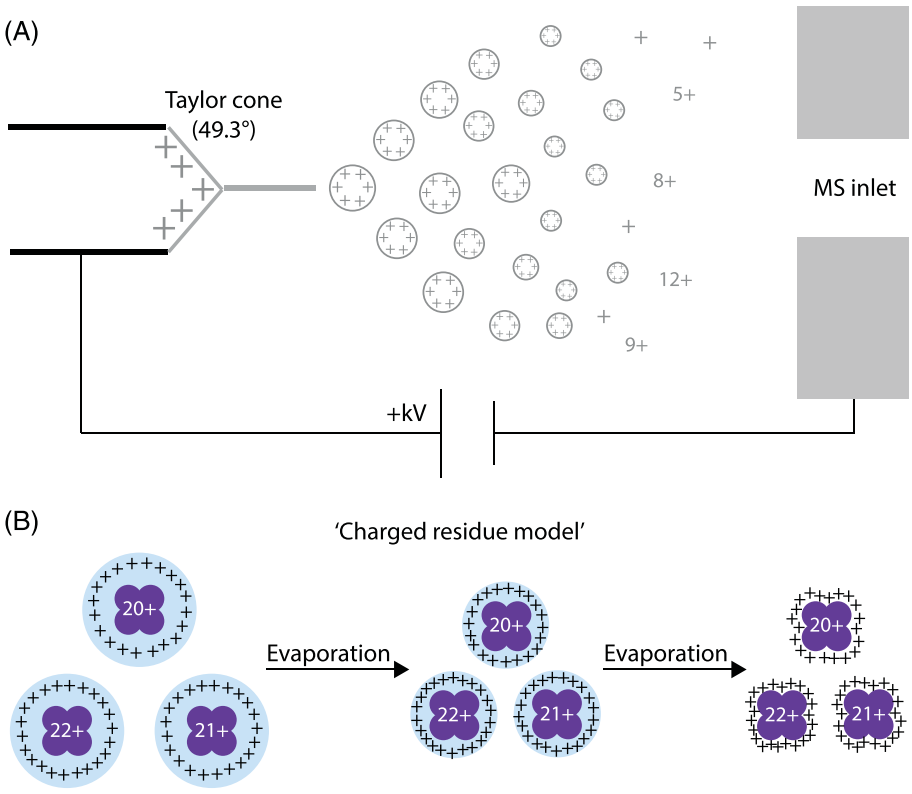

FIGURE 3 Transfer of proteins into the gas phase. (A) The ESI process. A spray of charged droplets is emitted from the ESI emitter. The ionisation process of molecules differing in size from charged droplets is explained by different models. See text for details. (B) Ionisation of folded proteins and protein complexes is explained by the charged residue model. Upon evaporation, the charges are transferred to the molecule ion. The charges correlate with the surface of a globular protein of similar size

5 | NATIVE MS AND TANDEM MS EXPERIMENTS

In standard native MS experiments, the protein solution is sprayed through an ESI emitter, and obtained ions of the proteins or protein complexes are detected in the mass spectrometer. In these experiments, the quadrupole mass analyser is operated in 'scanning mode', that is, the full range of ions is transmitted. The acquired mass spectra show mass-to-charge (m/z) ratios of the intact complexes that can be deconvolved to obtain the masses of the complexes. When multiple complexes or proteins are present in solution and the resolution of the mass spectrometer is sufficient to separate the different complexes, they are all observed in the same mass spectrum. Native MS therefore also provides information on homogeneity or heterogeneity of the assemblies (Figure 4A).

Similar to other MS applications, a precursor ion can be isolated in the quadrupole and dissociated in tandem MS experiments (Figure 4B). For this, collision-induced dissociation (CID) is usually employed. While CID of proteins or peptides causes their fragmentation, dissociation of a protein complex's precursor ion yields, with few exceptions, an unfolded, highly charged monomer and a so-called 'stripped' complex comprising the remaining subunits.[48–50] The charges of the precursor ion are therefore asymmetrically distributed between the dissociated monomer and the stripped complex. Similar results are obtained from higher energy collision dissociation (HCD), which is applied when using Orbitrap mass spectrometers.[51]

6 | MASS SPECTRA OF INTACT PROTEIN COMPLEXES REVEAL THEIR STRUCTURAL ARRANGEMENTS

In accordance with the charged residue model (see Section 4 and Figure 3B), native mass spectra of folded proteins or protein complexes show a series of few charge states with Gaussian distribution (Figure 5). The number of acquired charges usually correlates with the surface area of the globular protein. Observing a distribution of several charge states of the species allows calculating the molecular weight of the protein complex from two neighbouring peaks with m/z ratios of $(m^{\text{Protein}} + z{\cdot}m^{\text{Proton}})/z$ and $(m^{\text{Protein}} + (z+1){\cdot}m^{\text{Proton}})/(z+1)$, where z is the number of charges (i.e., protons) that differs by one between the two neighbouring charge states (Figure 5). To facilitate annotation of native MS spectra and calculation of molecular masses of protein-ligand assemblies, several deconvolution software tools have been developed; these include MaxEnt,[52] Massign,[53] UniDec,[54] PeakSeeker[55] or Intact Mass™[56,57] (see Allison et al[58] for a complete summary). However, in most cases, annotation of peak series is semi-automated, and manual evaluation is required. Note that during native MS, the experimentally determined mass of a protein or protein complex is usually higher than its theoretical mass. This mass shift is caused by incomplete desolvation and remaining buffer and salt adducts. In contrast to a folded protein, a protein that is denatured in solution shows a larger distribution of charge states with higher charges. The observed charge states in native MS spectra are therefore indicative

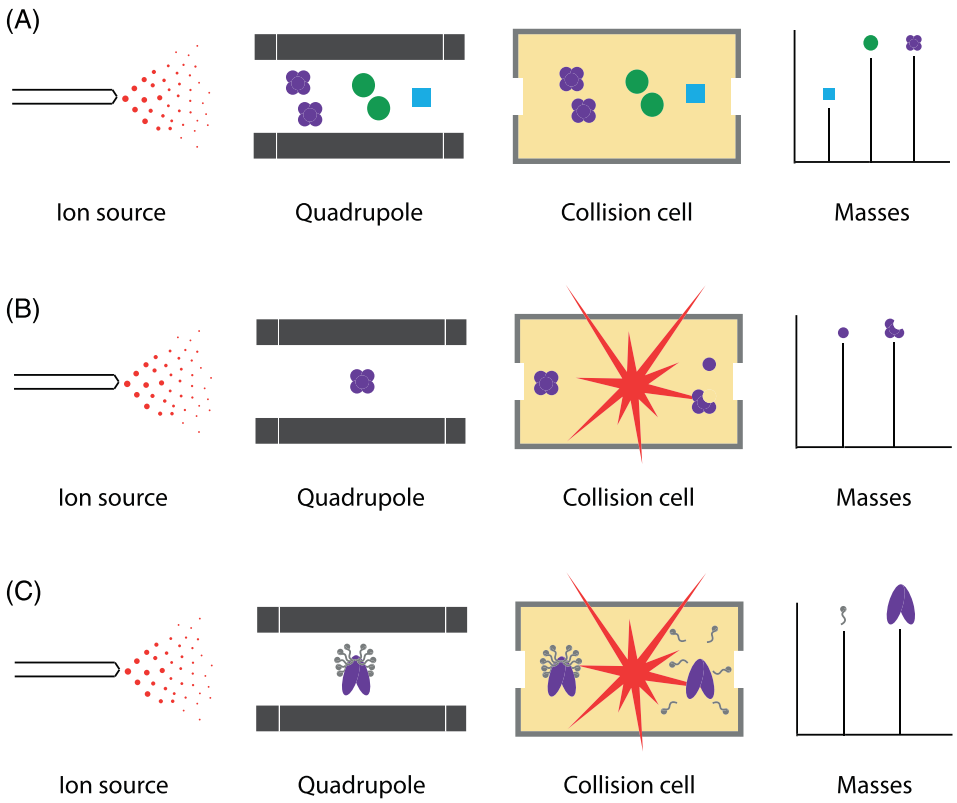

FIGURE 4 Native MS experiments. (A) MS experiment. Ions are generated by ESI. The quadrupole mass analyser allows transmission of all m/z's. Masses of all proteins and protein complexes are determined by deconvolution from the observed mass spectrum. (B) Tandem MS experiment. The quadrupole mass analyser allows transmission of one specific m/z. The collision cell is operated at higher collisional voltage causing dissociation of a highly charged monomer. The masses of the monomeric subunit and the remaining stripped complex are obtained from the mass spectrum. (C) Native MS of a membrane protein. The quadrupole mass analyser allows transmission of all m/z's. The collision cell is operated at higher collisional voltage causing dissociation of the detergent micelle and releasing the membrane protein

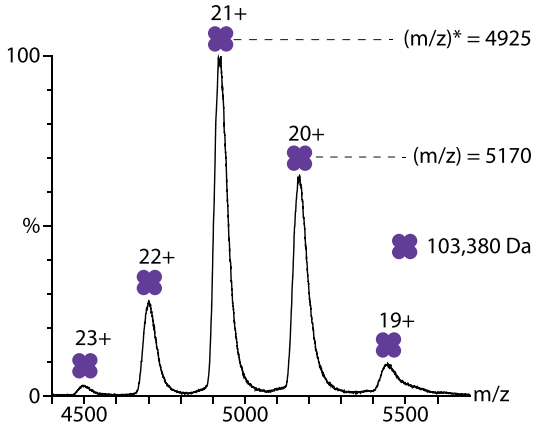

$$(m/z)^* = \frac{m^{Protein} + (z+1)\cdot m^{Proton}}{(z+1)}$$

$$(m/z) = \frac{m^{Protein} + z\cdot m^{Proton}}{z}$$

$$(m/z) > (m/z)^* \quad \text{and} \quad m^{Proton} \approx 1$$

$$z(m/z) = \frac{(m/z)^* - 1}{(m/z) - (m/z)^*}$$

$$m^{Protein} = z\cdot(m/z - 1)$$

FIGURE 5 Typical native MS spectrum of tetrameric concanavalin A. A Gaussian distribution of charge states (19+ to 23+) is observed. The molecular weight of the protein complex can be calculated from two neighbouring *m/z* ratios using the given equations (rhs). The molecular weight of 103 380 Da was calculated for the concanavalin A tetramer

for the folding state of the proteins/protein complexes, that is, folded or unfolded states.

In many cases, proteins and protein complexes interact with ligands, for instance, nucleotides, lipids or sugars. For these complexes, a mass shift corresponding to the mass of the ligand is observed for all charge states. For ligands that stoichiometrically bind the protein complex, this mass shift is observed for the entire population; substoichiometric binding of ligands is unveiled by the presence of peak populations corresponding to the apo- and ligand-bound forms (see Figure 6A for an example).

When collisional voltages in the range of 30–70 V are applied during native tandem MS, dissociation is usually observed for one peripheral subunit (see Figure 6B for an example). Note that several dissociation processes can take place in parallel yielding a set of dissociation products. Tandem MS spectra therefore reveal peripheral subunits and thus provide information on the structural arrangements of protein complexes. An alternative dissociation technique that has also been developed for protein complexes is surface induced dissociation (SID).[60,61] During SID, multi-subunit complexes dissociate into smaller subcomplexes of few subunits.[62,63] Symmetrical distribution of charges between these subcomplexes gave rise to the assumption that dissociated subcomplexes are folded; this could be confirmed by further experiments.[63–65]

To gain additional information on the protein complex' architecture, intact protein complexes can be dissociated in solution by addition of organic solvents or acids.[6,66] Following this approach, stable interaction modules of the protein complexes are observed in the mass spectrum, which can further be analysed by tandem MS as described above. This strategy is particularly promising when studying multi-subunit assemblies such as the human eukaryotic initiation factor 3 comprising 13 subunits[67] or various CRISPR complexes comprising few subunits in varying stoichiometries.[68,69]

7 | THE CHALLENGE OF ANALYSING LARGE MACROMOLECULAR ASSEMBLIES BY NATIVE MS

Since the first developments of native MS, the analysis of macromolecular, multi-subunit protein assemblies was one of the major goals.

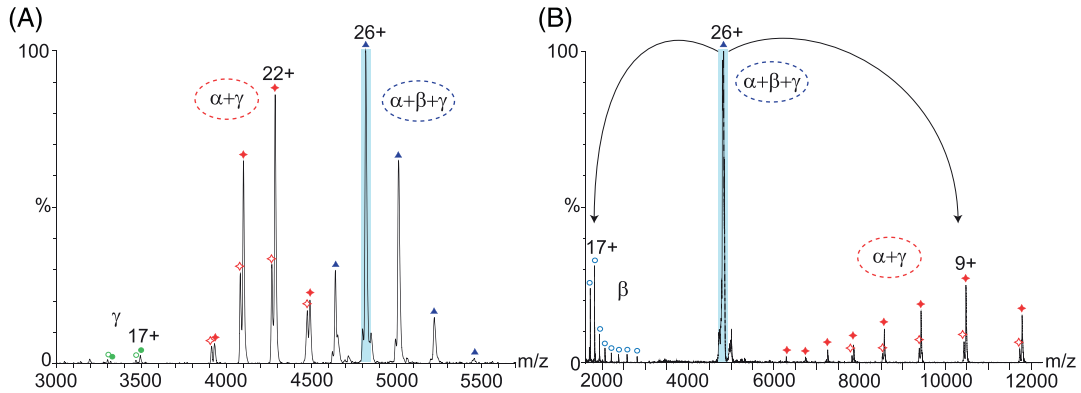

FIGURE 6 Native MS spectrum of trimeric eIF2. (A) MS spectrum. The trimeric complex ($\alpha + \gamma + \beta$, blue triangles) as well as a dimeric complex ($\alpha + \gamma$, red diamonds) and the monomeric γ subunits (green circles) are observed. The trimeric complex stoichiometrically binds GTP. The dimeric complex substoichiometrically binds GTP (filled *versus* unfilled diamonds). The γ subunit substoichiometrically binds GTP (filled and unfilled red circles). (B) Tandem mass spectrum. The 26+-charge state of trimeric eIF2 (blue triangle) was selected in the quadrupole. A stripped complex, which lost the β subunit was observed at high *m/z* (filled and unfilled red diamonds). The highly charged β subunit was assigned in the low *m/z* region (unfilled light-blue circles). The charges of the dissociated β subunit and the stripped complex add up to the initial charge of the selected precursor (17 + 9 = 26). The figure was partially adapted from Gordiyenko et al[59] under the CC BY 3.0 license

Among the first targets were ribosomes, which presented a major challenge for native MS in terms of high-mass instrumentation and data analysis. Ribosomes are large protein-RNA machineries that translate messenger-RNA into proteins in all living cells. The small and large ribosomal subunits assemble on the messenger-RNA resulting in intact 70S and 80S ribosomes in bacteria or eukaryotes, respectively. Despite size and complexity, mass spectra of ribosomes from various species including *Escherichia coli*,[70] *Saccharomyces cerevisiae*[71] and *Thermus thermophilus*[72] were acquired. Even though the resolution of these mass spectra was limited at that time, series of charge states could be assigned to the small and large ribosomal subunits as well as intact ribosomes (see Figure 7A for an example). Later studies took advantage of MS and focused on the analysis of ribosomal stalk complexes that extrude from the large ribosomal subunit and were, due to their dynamic nature, difficult to study by X-ray crystallography (Figure 7B).[71,75,76] MS consequently allowed determination of stalk complex' stoichiometries of ribosomes from various species and in different growth phases.

The largest assemblies studied by native MS to-date are viruses which reach molecular weights up to several megadaltons in their DNA-filled forms. Their well-ordered and stable arrangement of only few capsid proteins makes them an ideal model system. However, due to their large size, complexity of assembly intermediates and dynamics in solution ('capsid breathing'), their analysis by native MS remains challenging.[77] In an early study, an intact virus was successfully transferred into the gas phase of a mass spectrometer;[78] however, an actual mass analysis could not be performed with the unmodified instrument employed in this study. Two decades later and using a modified Q-ToF mass spectrometer (see Section 3), well-resolved spectra of hepatitis B virus capsids allowed the assignment of two capsid morphologies of 3 and 4 MDa, respectively (Figure 7C).[74] Further improvements and developments advanced the application of native MS to study viruses; accordingly, exchange dynamics,[79] capsid stability[80,81] or ligand binding (e.g., carbohydrate binding)[82,83] is nowadays accessible. Recent developments in high-resolution native MS instrumentation even allowed the distinction between virus particles that differed in cargo loading and capsid composition.[84,85]

8 | UNRAVELLING THE ARCHITECTURE OF MEMBRANE PROTEIN ASSEMBLIES AND LIPID BINDING

Specific to all integral membrane proteins is their requirement for a membrane-like environment to maintain solubility after extraction from the natural membrane environment. This is in most cases achieved by employing membrane mimetics. The simplest membrane mimetic is a detergent micelle; due to their structural properties, detergents form micelles in solution and arrange around the hydrophobic transmembrane domains of integral membrane proteins.[86] The association of detergent molecules, however, hampers the analysis by MS and causes severe peak broadening or ion suppression.[87,88] To overcome this problem, membrane proteins or protein complexes are released from the detergent micelle by CID in the gas phase of the

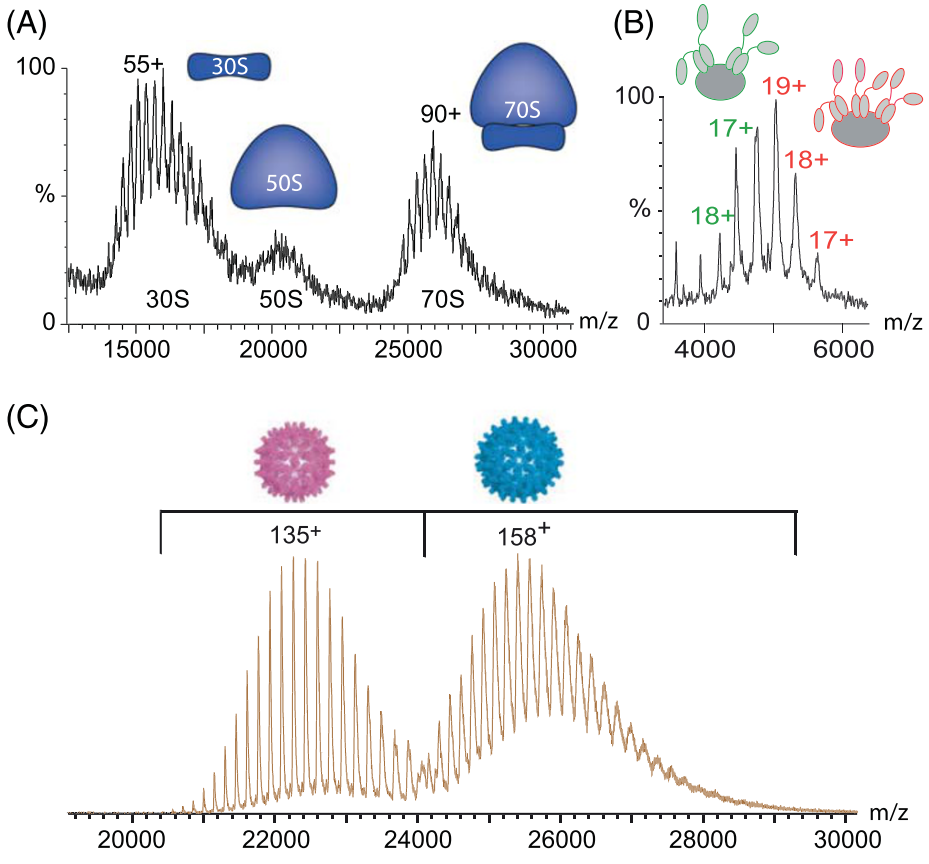

FIGURE 7 Native MS of large macromolecular assemblies. (A) Native mass spectrum of ribosomes from *Thermus thermophilus*. Intact 70S ribosomes as well as 30S and 50S small and large ribosomal subunits were observed. Panel A adapted from Schmidt et al[73] under the CC BY 4.0 license. (B) Populations of stalk complexes differing in protein stoichiometry were observed for mesophilic archaea. Figure adapted from Schmidt et al[73] under the CC BY 4.0 license. (C) Native MS spectrum of hepatitis B virus. Two charge state distributions corresponding to capsids of 3 (red) and 4 (blue) MDa were observed. Panel B adapted from Uetrecht et al[74] Copyright 2008 National Academy of Sciences

mass spectrometer[89,90] (Figure 4C). A similar effect is observed by reducing collisional cooling in the ion source.[91] However, the required energy to release the intact membrane proteins from the detergent micelle is often too high causing unfolding of the proteins or dissociation of protein subunits from the intact assemblies. Screening a variety of MS-compatible detergents followed by fine-tuning of instrument parameters is therefore recommended to determine ideal conditions for native MS experiments of membrane proteins.[92,93] Recent developments therefore include the design of specialised detergents for native MS analysis.[94]

ATP synthases (ATPases) were among the first membrane protein assemblies to be studied by native MS.[95] They are multi-subunit protein complexes containing a large soluble domain and a multimeric membrane ring connected through a central stator stalk and stabilised by peripheral stalk complexes.[96,97] ATP synthases utilise a proton gradient for ATP synthesis while ATPases hydrolyse ATP and thereby establish a proton gradient.[98] The first study targeted the *Thermus thermophilus* ATPase/Synthase.[95] Even though the detergent micelle caused severe peak broadening, selection of a wider *m/z* region yielded well-resolved stripped complexes of defined stoichiometry. Later improvements in sample preparation and instrument tuning[89,90] then allowed the analysis of intact ATPases and revealed stoichiometries, subunit interactions and lipid binding[99,100] as well as complex stability in response to removal of post-translational modifications.[101,102] An example spectrum of an intact ATP synthase is shown in Figure 8.

In addition to ATP synthases, many membrane transporters and channels have been analysed. Most of these proteins are small homo- or hetero-oligomers with large hydrophobic domains embedded in the lipid bilayer. Early studies mainly focussed on the methodological advances to study protein stoichiometries and binding of associated lipids.[90,103] However, recent improvements enabled the analysis of cooperative binding of lipids, drugs or other ligands such as nucleotides or peptides.[104,105] Importantly, native MS directly reveals the effects of lipid binding onto the stability and formation of protein complexes.[106–108]

Due to several drawbacks of detergent micelles, other membrane mimetics that better resemble the lipid bilayer of biological membranes are favoured and explored.[109] However, these are usually more complex including phospholipids and scaffold proteins or polymers.[110,111] A first study explored nanodiscs, bicelles and amphipols for native MS and showed that indeed the native oligomeric states of several integral membrane proteins were preserved in nanodiscs and bicelles while they differed from those obtained from detergent micelles or amphipols.[112] In particular, nanodiscs were therefore examined in detail; the complex and heterogeneous mass spectra further induced improvements in spectral deconvolution,[113–116] sample preparation[117–119] and method optimisation.[119,120] These

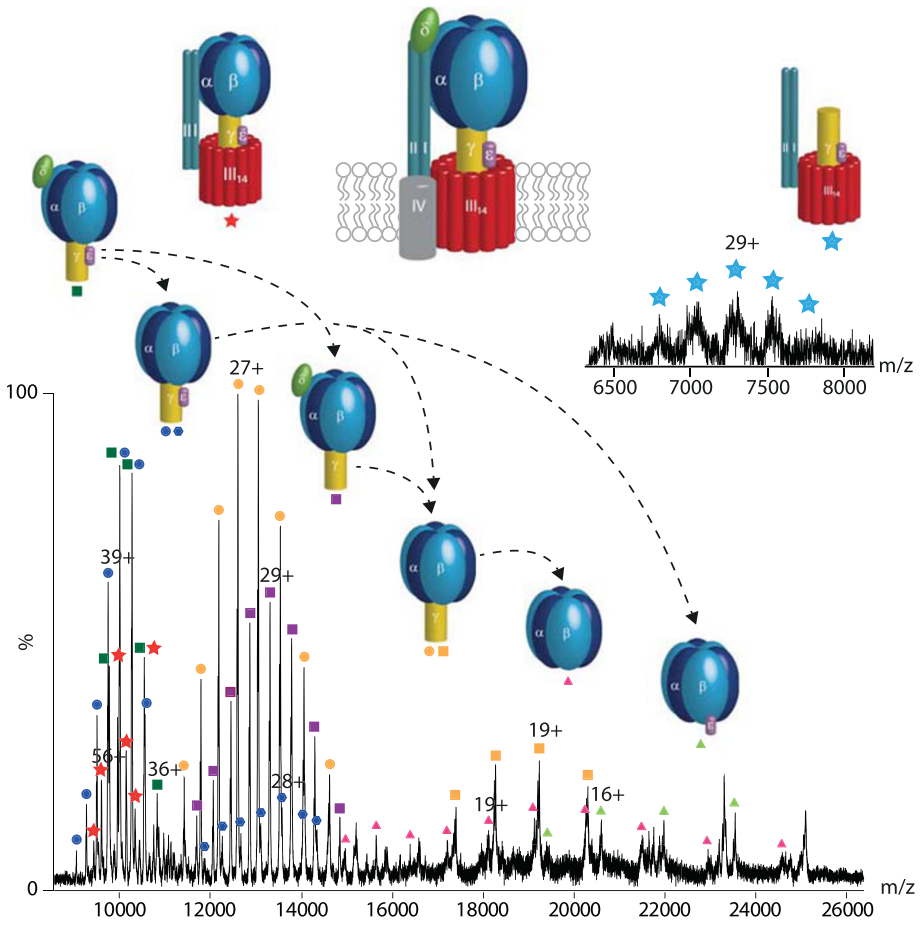

FIGURE 8 Native MS of an ATP synthase. The native mass spectrum shows several complexes that dissociated in solution (9000–10 000 *m/z*). The high energy required to release the complex from the detergent micelle caused dissociation of peripheral subunits and revealed first (12 000–14 000 *m/z*) and second (17 000–25 000 *m/z*) generation CID products. The inset shows a subcomplex containing the membrane ring. Figure adapted from Schmidt et al[101] under the CC BY 3.0 license

improvements allowed, for instance, monitoring the insertion and oligomer assembly in the lipid bilayer.[120,121]

A recent breakthrough was the analysis of intact protein-ligand assemblies directly from native membranes.[122,123] For this, native membranes were purified and subsequently sonicated in ammonium acetate to reduce integrity; they were then directly analysed by native MS. Following this approach, respiratory chain complexes of mitochondrial membranes as well as transporters and the SecYEG translocon from *E. coli* inner membranes were, amongst others, identified and assigned. The identification of many interactions with ligands of these proteins reveals the importance of the native membrane for maintaining these interactions.[122]

9 | ASSESSING PROTEIN SHAPE AND STABILITY THROUGH NATIVE IM-MS

IM is a tool for separation of complex ion mixtures in the gas phase.[124,125] It is routinely applied as an analytical technique in the fields of drug and explosive detection as well as pharmaceutical and food industry. The coupling of IM and native MS provides additional structural information on size, shape and stability of proteins or protein-ligand complexes. The first step of a native IM-MS experiment is ionisation of the proteins by nano-ESI and subsequent transfer of the ions into a modified mass spectrometer (see Sections 3 and 4). In the mass spectrometer, the ions are guided through an IM cell[126,127] preceded or followed by MS or tandem MS analysis. Four IM-MS techniques are mainly used: drift-time ion mobility (DTIM) MS, travelling wave ion mobility (TWIM) MS, trapped ion mobility (TIM) MS and field asymmetric ion mobility spectrometry (FAIMS). Of these, the latter is primarily employed to filter out unwanted interferences at atmospheric pressure.[128] While it is increasing specificity and sensitivity for the subsequent MS analysis, the major disadvantage of FAIMS in respect of protein complex' analysis is that information on the structure of the analytes is not obtained.[129] This rather specialized technique will therefore not be discussed in detail.

DTIM is the traditional form of IM. Separation of ions is achieved by passing the ions through a drift tube containing an inert buffer gas.[130] A uniform electric field gradient is applied along the drift tube propelling the ions in the direction of the applied field. The drift time of the ions through the drift tube is related to their shape, providing information on their collision cross section (CCS). In detail, compact, smaller structures experience fewer collisions with the buffer gas and therefore travel faster than elongated structures (Figure 9A). From

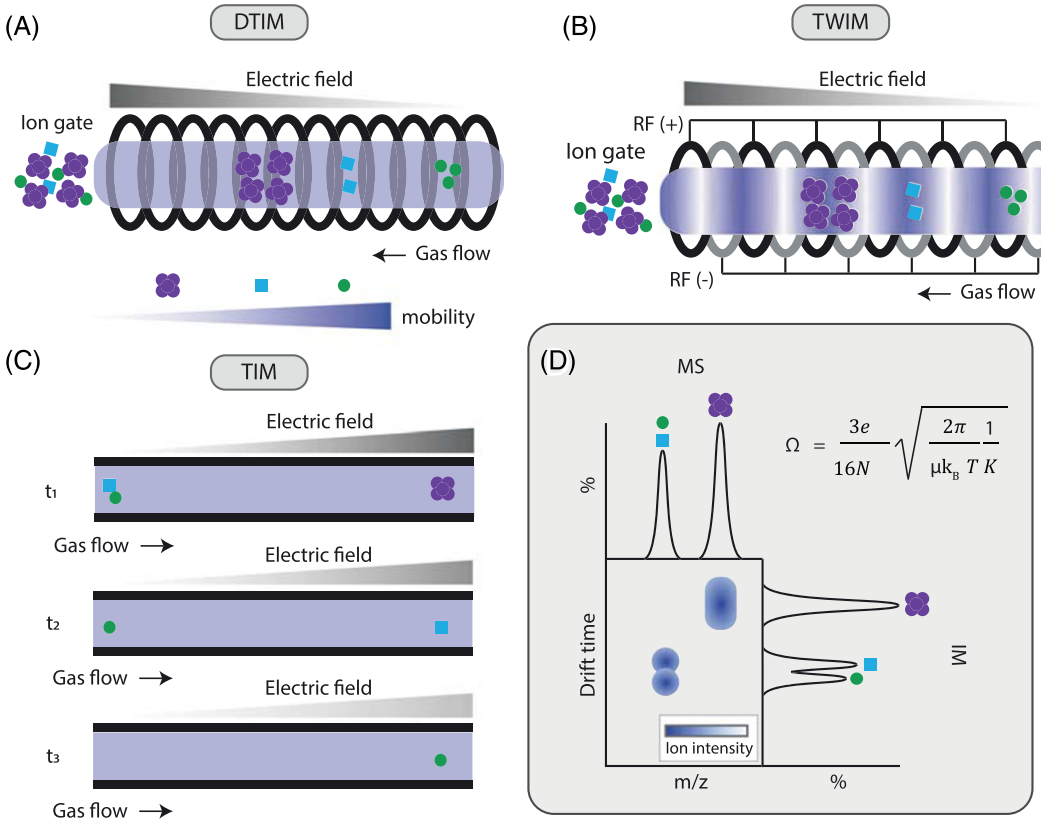

FIGURE 9 Native IM-MS of protein complexes. (A) Basic principle of DTIM. Ions are accelerated in a counter gas flow. According to their shape, they undergo more (larger ions) or fewer (smaller ions) collisions. (B) Basic principle of TWIM. A traveling voltage wave is applied. Smaller ions are carried with the wave and larger ions are retained. (C) Basic principle of TIM. Ions are trapped in the IM cell. When decreasing the electric field strength ($t_1 > t_2 > t_3$), the ions are carried along the drift tube by the IM gas. Larger ions undergo more collisions and are released first. (D) IM drift plot. Ions with the same *m/z* but differing in shape are separated by IM and are observed at different drift times. The CCSs of ions are calculated using the Mason-Schamp equation

recorded arrival time distribution at the detector, drift time distributions through the IM cell are obtained which are then used to calculate the CCS following the Mason-Schamp equation.[131]

During TWIM, a travelling voltage wave is applied to a series of electrically connected ring electrodes pushing the ions through the IM cell.[132] This 'travelling wave' is created by the application of a transient direct current voltage pulse to each electrode located at both ends of the IM tube.[132] Smaller, compact ions with higher mobility are carried by the travelling wave, while bigger, elongated structures with lower mobility are slower (Figure 9B). Differential separation of a complex mixture is obtained by optimizing velocity and height of the travelling wave. Improved resolution in TWIM can be achieved by multipass cyclic IM[133]; this has successfully been applied to separate conformers of monomeric and tetrameric proteins.[134] The CCSs of the analyte ions are calculated after calibration of the drift time with similar ions of known CCS and charge state.[135,136] For this, a set of standard proteins is available for which CCSs are obtained from DTIM experiments.[136] By acquiring arrival time distributions of the calibrants at varying travelling wave height and velocity, a calibration curve of CCSs is obtained and applied to proteins and protein complexes with unknown CCS.[137] Of note, calibrants and analytes should be comparable in terms of mass, shape and charge states. Calibration of drift time measurements is also advised for DTIM if gas purity, pressure and temperature are not stable or cannot be recorded accurately. Different software was developed and is often applied to automate the calibration process and to calculate CCSs from arrival time distributions.[138–141] Note that the requirement for calibration increases the analysis time when using TWIM.

Recently, TIM was introduced.[142,143] During TIM, the ions are trapped by an electrostatic force and a flow of buffer gas in opposite directions.[144,145] When decreasing the strength of the electric field, the ions are "pushed" forward by the buffer gas and are released from the IM cell (Figure 9C). When compared with other IM techniques, analytes with low mobility and extended shape are released first because they undergo more collisions with the buffer gas. Similar to TWIM, the CCS is then determined after calibration.[145–148]

IM adds another dimension of separation during native MS analysis of proteins and protein complexes; ions with the same *m/z* but differing in shape can be distinguished and structurally characterized (Figure 9D). A key finding was the observation that the ring structure of the tRNA binding protein TRAP was maintained in the gas phase evidencing the applicability of native IM-MS for studying protein complex structures.[127] The structural interpretation of obtained drift times and CCSs of proteins and protein complexes mostly relies on molecular modelling approaches.[149,150] One possible procedure is to calculate CCS values for candidate models and compare them with experimentally obtained CCS values.[151] Several algorithms are employed in specialized software to calculate CCSs from models. They are based on projection approximation,[152–154] projection superposition approximation,[155–158] local collision probability approximation,[159] exact hard spheres scattering,[160,161] scattering on electron density isosurfaces[162] or trajectory methods.[163,164]

Another application of native IM-MS is collision-induced unfolding to analyse the conformational stability of a protein complex under different conditions.[139,165–167] For this, the collisional energy is increased leading to collisional activation and sequential unfolding of the protein. The unfolding process of the protein is then monitored by an increase in CCS. For visualization of changes in protein or protein complex stability, unfolding plots are generated manually or using specialised software.[138–140,168,169] These plots allow a comparison of activation levels and transition states of the proteins or protein complexes under varying conditions. Collision-induced unfolding has successfully been applied to study the effects of ligands, for instance, binding of substrates and co-factors[170–172] or associated lipids,[139,173] onto protein stability.

As a consequence of the variety of IM techniques, the application of native IM-MS is diverse. It ranges from building structural models to functional studies. Prominent examples are epitope mapping utilising IM separation to identify antigen-epitope complexes[174–176] or fibril and amyloid formation.[177–180] Recent improvements in sample preparation (see Section 2) even allow the native IM-MS analysis of proteins from cell lysates.[21]

10 | RECENT ADVANCES ENABLE HIGH-RESOLUTION NATIVE MS

Sample preparation, instrumentation and data analysis of native MS were continuously improved over the last two decades. A major breakthrough was the establishment of high-resolution mass spectrometers modified for transmission of high-mass complexes. The first modifications were conducted on an Exactive Plus Orbitrap mass spectrometer and included software modifications allowing detection of high-mass ions up to 24 000 *m/z*, tuning radiofrequencies of transport multipoles and increased pressure in the HCD cell.[181] In detail, maximum radiofrequency voltages were applied to all RF multipoles allowing transmission of high-mass ions. For better desolvation and increased sensitivity, the ions were trapped in the HCD cell instead of the C-trap. A new gas line allowed switching between different collision gases and manual pressure adjustments in the range of 5×10^{-10} and 2×10^{-9} mbar. Additional desolvation was induced by applying in-source dissociation energy. Mass filtering of ions was optimised by manually tuning voltages of multipoles and lenses. Using this instrument, highly resolved mass spectra of an IgG antibody, the 20S proteasome, bacteriophage capsid complexes and GroEL chaperone were recorded resulting in masses of the complexes within 10–50 ppm accuracy.[181]

The developments of high-resolution instrumentation were then pursued on a Q Exactive hybrid quadrupole-Orbitrap mass spectrometer and included, as described above for Q-ToF instruments, lower radiofrequency of the quadrupole to allow precursor mass selection up to 20 000 *m/z*, a modified preamplifier for detection of high-mass signals and changes in the HCD-gas inlet to achieve even higher pressures up to 1×10^{-9} mbar.[182] Figure 10A shows a schematic of the modified mass spectrometer. Using this instrument and additionally

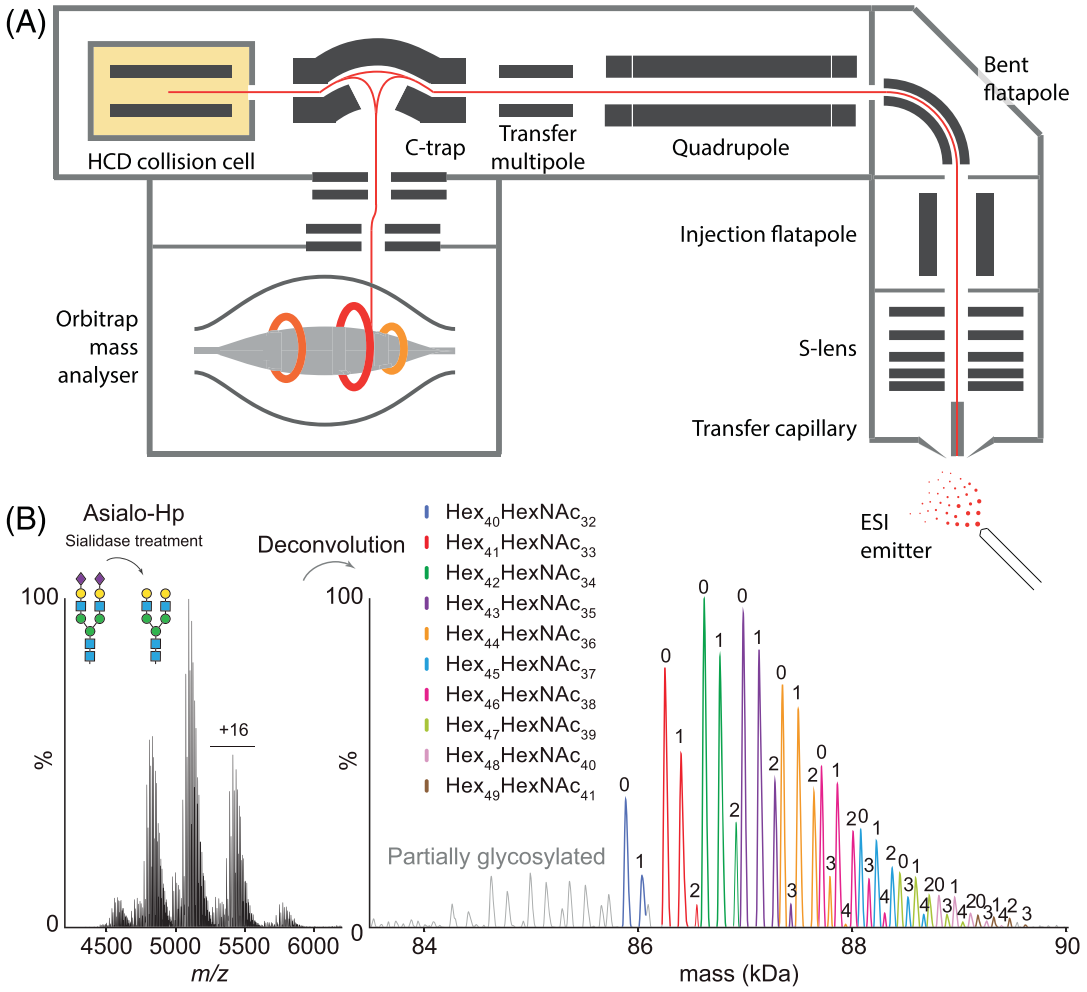

FIGURE 10 High-resolution native MS. (A) Schematic of a Q Exactive hybrid quadrupole-Orbitrap mass spectrometer. Relevant elements and components are shown. Ions are generated by ESI. The ion beam (red) is shown throughout the instrument. See text for details on instrument modifications. (B) High-resolution mass spectrum of Asialo-HP glycoprotein (lhs). Deconvolution of the mass spectrum reveals the microheterogeneity of Asialo-HP (rhs). Peaks corresponding to the same hexose composition are highlighted (see colour legend). The number of fucose residues is indicated for each peak. Panel B adapted from Wu et al[183] under the CC BY-NC 3.0 license

tuning of voltage gradients then allowed the protection of membrane protein complexes by the detergent micelles, which was removed by collisional dissociation in the HCD cell. Following this procedure, high-resolution native MS was extended by the analysis of membrane protein-ligand complexes. Strikingly, binding of associated lipids, detergent molecules and small molecule drugs could be resolved and revealed binding stoichiometries and preferences for endogenous lipids that differ in acyl chain length.[182]

Continuous improvements in high-resolution instrumentation followed. The establishment of a Q Exactive ultra-high mass range spectrometer (QE-UHMR) extended the mass range dramatically for the analysis of large macromolecular complexes up to 50 000 *m/z* as exemplified by the 9-MDa Flock House virus.[184] Another instrument modification included the addition of a dual funnel interface allowing the detection of an intact protein complex without in source activation and at lower collisional energies.[185] This instrumental set-up enabled complete desolvation and dissociation of the protein complex in the front-end of the mass spectrometer, between dual funnel and injection flatapole, providing the possibility of pseudo-MS3 experiments for fragmentation of monomer subunits.[185,186] Recently, the range of high-resolution instrumentation was further extended by tribrid mass spectrometers allowing multistage activation and thereby dissociation and subsequent fragmentation of bound ligands.[187] This approach is crucial for unambiguously linking ligands with their target proteins.

The possibility of high-resolution native MS revolutionised the field of native MS and extended its applications enormously. To name a few examples, lipid binding to various membrane proteins,[188,189] heterogeneous populations of post-translationally modified proteins,[183,190,191] virus particles differing in genome content and capsid composition[84,85] and many other proteins and protein complexes have been explored to-date. A high-resolution mass spectrum revealing the microheterogeneity of Asialo-HP glycoprotein is shown in Figure 10B as an example. Very recently, high-resolution native MS and IM were successfully coupled allowing separation of the gas phase structures of highly resolved protein complex' populations.[192] In future, many more applications of high-resolution native MS are anticipated.

11 | CONCLUSIONS

Native MS has emerged as a robust method to determine the stoichiometry of protein complexes and protein-ligand assemblies. However, native MS is a versatile technique and, in addition to this rather simple application, provides information on protein(-ligand) interactions, complex' heterogeneity and topology. The establishment of high-resolution instrumentation nowadays allows taking snapshots of co-existing populations of protein-ligand complexes thereby uncovering mechanistic details and synergistic effects. When combined with IM, native MS delivers insights into complex' shape and stability of the proteins under different conditions. Together with biochemical or biophysical techniques, native MS provides invaluable information that is often difficult to achieve with the classical techniques alone. It therefore takes an important role in structural biology and future developments raise high expectations for further applications.

ACKNOWLEDGEMENTS

We thank Di Wu and Carol Robinson (both Oxford University), Yuliya Gordiyenko (MRC Laboratory of Molecular Biology, Cambridge), Albert Heck (Utrecht University) and Charlotte Uetrecht (Heinrich Pette Institute, Hamburg) for providing mass spectra of Figures 6, 7 and 10. We thank all group members for fruitful discussions and Julia Hesselbarth and Melissa Frick for comments on the manuscript. We acknowledge funding from the Federal Ministry for Education and Research (BMBF, ZIK programme, 03Z22HN22), the European Regional Development Funds (EFRE, ZS/2016/04/78115) and the Martin Luther University Halle-Wittenberg.

ORCID

Carla Schmidt https://orcid.org/0000-0001-9410-1424

REFERENCES

1. Karas M, Bachmann D, Bahr U, Hillenkamp F. Matrix-assisted ultraviolet laser desorption of non-volatile compounds. *Int J Mass Spectrom Ion Process*. 1987;78:53-68.
2. Tanaka K, Waki H, Ido Y, et al. Protein and polymer analyses up to *m/z* 100 000 by laser ionization time-of-flight mass spectrometry. *Rapid Commun Mass Spectrom*. 1988;2(8):151-153.
3. Fenn JB, Mann M, Meng CK, Wong SF, Whitehouse CM. Electrospray ionization for mass spectrometry of large biomolecules. *Science (New York, NY)*. 1989;246(4926):64-71.
4. Schmidt C, Robinson CV. Dynamic protein ligand interactions—insights from MS. *FEBS J*. 2014;281(8):1950-1964.
5. Mehmood S, Allison TM, Robinson CV. Mass spectrometry of protein complexes: from origins to applications. *Annu Rev Phys Chem*. 2015;66(1):453-474.
6. Hernandez H, Robinson CV. Determining the stoichiometry and interactions of macromolecular assemblies from mass spectrometry. *Nat Protoc*. 2007;2(3):715-726.
7. Pan P, McLuckey SA. The effect of small cations on the positive electrospray responses of proteins at low pH. *Anal Chem*. 2003;75(20):5468-5474.
8. Ikonomou MG, Blades AT, Kebarle P. Investigations of the electrospray interface for liquid chromatography/mass spectrometry. *Anal Chem*. 1990;62(9):957-967.
9. Clarke DJ, Campopiano DJ. Desalting large protein complexes during native electrospray mass spectrometry by addition of amino acids to the working solution. *Analyst*. 2015;140(8):2679-2686.
10. Cassou CA, Williams ER. Desalting protein ions in native mass spectrometry using supercharging reagents. *Analyst*. 2014;139(19):4810-4819.
11. Iavarone AT, Udekwu OA, Williams ER. Buffer loading for counteracting metal salt-induced signal suppression in electrospray ionization. *Anal Chem*. 2004;76(14):3944-3950.
12. Gault J, Lianoudaki D, Kaldmae M, et al. Mass spectrometry reveals the direct action of a chemical chaperone. *J Phys Chem Lett*. 2018;9(14):4082-4086.
13. Olinares PD, Dunn AD, Padovan JC, Fernandez-Martinez J, Rout MP, Chait BT. A robust workflow for native mass spectrometric analysis of affinity-isolated endogenous protein assemblies. *Anal Chem*. 2016;88(5):2799-2807.
14. Verkerk UH, Kebarle P. Ion-ion and ion-molecule reactions at the surface of proteins produced by nanospray. Information on the number of acidic residues and control of the number of ionized acidic and basic residues. *J Am Soc Mass Spectrom*. 2005;16(8):1325-1341.
15. Konermann L. Addressing a common misconception: ammonium acetate as neutral pH "buffer" for native electrospray mass spectrometry. *J Am Soc Mass Spectrom*. 2017;28(9):1827-1835.
16. Waitt GM, Xu R, Wisely GB, Williams JD. Automated in-line gel filtration for native state mass spectrometry. *J Am Soc Mass Spectrom*. 2008;19(2):239-245.
17. Heck AJ. Native mass spectrometry: a bridge between interactomics and structural biology. *Nat Methods*. 2008;5(11):927-933.
18. Benkestock K, Edlund PO, Roeraade J. On-line microdialysis for enhanced resolution and sensitivity during electrospray mass spectrometry of non-covalent complexes and competitive binding studies. *Rapid Commun Mass Spectrom*. 2002;16(21):2054-2059.
19. Susa AC, Xia Z, Williams ER. Small emitter tips for native mass spectrometry of proteins and protein complexes from nonvolatile buffers that mimic the intracellular environment. *Anal Chem*. 2017;89(5):3116-3122.
20. Vimer S, Ben-Nissan G, Sharon M. Direct characterization of overproduced proteins by native mass spectrometry. *Nat Protoc*. 2020;15(2):236-265.
21. Gan J, Ben-Nissan G, Arkind G, et al. Native mass spectrometry of recombinant proteins from crude cell lysates. *Anal Chem*. 2017;89(8):4398-4404.
22. VanAernum ZL, Busch F, Jones BJ, et al. Rapid online buffer exchange for screening of proteins, protein complexes and cell lysates by native mass spectrometry. *Nat Protoc*. 2020;15(3):1132-1157.
23. Morris HR, Paxton T, Dell A, et al. High sensitivity collisionally-activated decomposition tandem mass spectrometry on a novel quadrupole/orthogonal-acceleration time-of-flight mass spectrometer. *Rapid Commun Mass Spectrom*. 1996;10(8):889-896.
24. Sobott F, Hernandez H, McCammon MG, Tito MA, Robinson CV. A tandem mass spectrometer for improved transmission and analysis of large macromolecular assemblies. *Anal Chem*. 2002;74(6):1402-1407.
25. Krutchinsky AN, Chernushevich IV, Spicer VL, Ens W, Standing KG. Collisional damping interface for an electrospray ionization time-of-flight mass spectrometer. *J Am Soc Mass Spectrom*. 1998;9(6):569-579.
26. Tahallah N, Pinkse M, Maier CS, Heck AJ. The effect of the source pressure on the abundance of ions of noncovalent protein assemblies in an electrospray ionization orthogonal time-of-flight instrument. *Rapid Commun Mass Spectrom*. 2001;15(8):596-601.
27. Rostom AA, Robinson CV. Detection of the intact GroEL chaperonin assembly by mass spectrometry. *J Am Chem Soc*. 1999;121(19):4718-4719.

28. Tolmachev AV, Udseth HR, Smith RD. Radial stratification of ions as a function of mass to charge ratio in collisional cooling radio frequency multipoles used as ion guides or ion traps. *Rapid Commun Mass Spectrom*. 2000;14(20):1907-1913.
29. Thomson BA. 1997 McBryde Medal Award Lecture Radio frequency quadrupole ion guides in modern mass spectrometry. *Can J Chem*. 1998;76(5):499-505.
30. Taylor GI. Disintegration of water drops in an electric field. *Proc Roy Soc Lond Math Phys Sci*. 1964;280(1382):383-397.
31. Wilm M, Mann M. Analytical properties of the nanoelectrospray ion source. *Anal Chem*. 1996;68(1):1-8.
32. Wilm M. Principles of electrospray ionization. *Mol Cell Proteomics: MCP*. 2011;10(7):M111.009407.
33. Konermann L, Ahadi E, Rodriguez AD, Vahidi S. Unraveling the mechanism of electrospray ionization. *Anal Chem*. 2013;85(1):2-9.
34. Iribarne JV, Thomson BA. On the evaporation of small ions from charged droplets. *J Chem Phys*. 1976;64(6):2287-2294.
35. Dole M, Mack LL, Hines RL, Mobley RC, Ferguson LD, Alice MB. Molecular beams of macroions. *J Chem Phys*. 1968;49(5):2240-2249.
36. Konermann L, Rodriguez AD, Liu J. On the formation of highly charged gaseous ions from unfolded proteins by electrospray ionization. *Anal Chem*. 2012;84(15):6798-6804.
37. Gatlin CL, Turecek F. Acidity determination in droplets formed by electrospraying methanol-water solutions. *Anal Chem*. 1994;66(5):712-718.
38. Mirza UA, Chait BT. Do proteins denature during droplet evolution in electrospray ionization? *Int J Mass Spectrom Ion Process*. 1997;162(1):173-181.
39. Wolynes PG. Biomolecular folding in vacuo!!!(?). *Proc Natl Acad Sci U S A*. 1995;92(7):2426-2427.
40. Steinberg MZ, Elber R, McLafferty FW, Gerber RB, Breuker K. Early structural evolution of native cytochrome c after solvent removal. *Chembiochem*. 2008;9(15):2417-2423.
41. Breuker K, McLafferty FW. Native electron capture dissociation for the structural characterization of noncovalent interactions in native cytochrome C. *Angew Chem Int Ed Engl*. 2003;42(40):4900-4904.
42. Breuker K, McLafferty FW. The thermal unfolding of native cytochrome c in the transition from solution to gas phase probed by native electron capture dissociation. *Angew Chem Int Ed Engl*. 2005;44(31):4911-4914.
43. Badman ER, Myung S, Clemmer DE. Evidence for unfolding and refolding of gas-phase cytochrome C ions in a Paul trap. *J Am Soc Mass Spectrom*. 2005;16(9):1493-1497.
44. Breuker K, McLafferty FW. Stepwise evolution of protein native structure with electrospray into the gas phase, 10^{-12} to 10^{2} s. *Proc Natl Acad Sci U S A*. 2008;105(47):18145-18152.
45. Steinberg MZ, Breuker K, Elber R, Gerber RB. The dynamics of water evaporation from partially solvated cytochrome c in the gas phase. *Phys Chem Chem Phys: PCCP*. 2007;9(33):4690-4697.
46. Wyttenbach T, Bowers MT. Structural stability from solution to the gas phase: native solution structure of ubiquitin survives analysis in a solvent-free ion mobility–mass spectrometry environment. *J Phys Chem B*. 2011;115(42):12266-12275.
47. Bakhtiari M, Konermann L. Protein ions generated by native electrospray ionization: comparison of gas phase, solution, and crystal structures. *J Phys Chem B*. 2019;123(8):1784-1796.
48. Boeri Erba E, Ruotolo BT, Barsky D, Robinson CV. Ion mobility-mass spectrometry reveals the influence of subunit packing and charge on the dissociation of multiprotein complexes. *Anal Chem*. 2010;82(23):9702-9710.
49. Benesch JL, Aquilina JA, Ruotolo BT, Sobott F, Robinson CV. Tandem mass spectrometry reveals the quaternary organization of macromolecular assemblies. *Chem Biol*. 2006;13(6):597-605.
50. Beardsley RL, Jones CM, Galhena AS, Wysocki VH. Noncovalent protein tetramers and pentamers with "*n*" charges yield monomers with *n*/4 and *n*/5 charges. *Anal Chem*. 2009;81(4):1347-1356.
51. Olsen JV, Macek B, Lange O, Makarov A, Horning S, Mann M. Higher-energy C-trap dissociation for peptide modification analysis. *Nat Methods*. 2007;4(9):709-712.
52. Ferrige AG, Seddon MJ, Green BN, Jarvis SA, Skilling J, Staunton J. Disentangling electrospray spectra with maximum entropy. *Rapid Commun Mass Spectrom*. 1992;6(11):707-711.
53. Morgner N, Robinson CV. Massign: an assignment strategy for maximizing information from the mass spectra of heterogeneous protein assemblies. *Anal Chem*. 2012;84(6):2939-2948.
54. Marty MT, Baldwin AJ, Marklund EG, Hochberg GK, Benesch JL, Robinson CV. Bayesian deconvolution of mass and ion mobility spectra: from binary interactions to polydisperse ensembles. *Anal Chem*. 2015;87(8):4370-4376.
55. Lu J, Trnka MJ, Roh SH, et al. Improved peak detection and deconvolution of native electrospray mass spectra from large protein complexes. *J Am Soc Mass Spectrom*. 2015;26(12):2141–2151. https://10.1007/s13361-015-1235-6
56. Bern M, Caval T, Kil YJ, et al. Parsimonious charge deconvolution for native mass spectrometry. *J Proteome Res*. 2018;17(3):1216-1226.
57. https://www.proteinmetrics.com/products/intact-mass/
58. Allison T, Barran P, Benesch J, et al. Software for the analysis and interpretation of native mass spectrometry data. 2019, bioRxiv https://doi.org/10.26434/chemrxiv.11440254.v1
59. Gordiyenko Y, Schmidt C, Jennings MD, Matak-Vinkovic D, Pavitt GD, Robinson CV. eIF2B is a decameric guanine nucleotide exchange factor with a $\gamma_2\varepsilon_2$ tetrameric core. *Nat Commun*. 2014;5(1):3902.
60. Mabud MA, Dekrey MJ, Graham Cooks R. Surface-induced dissociation of molecular ions. *Int J Mass Spectrom Ion Process*. 1985;67(3):285-294.
61. Wysocki VH, Joyce KE, Jones CM, Beardsley RL. Surface-induced dissociation of small molecules, peptides, and non-covalent protein complexes. *J Am Soc Mass Spectrom*. 2008;19(2):190-208.
62. Blackwell AE, Dodds ED, Bandarian V, Wysocki VH. Revealing the quaternary structure of a heterogeneous noncovalent protein complex through surface-induced dissociation. *Anal Chem*. 2011;83(8):2862-2865.
63. Zhou M, Wysocki VH. Surface induced dissociation: dissecting noncovalent protein complexes in the gas phase. *Acc Chem Res*. 2014;47(4):1010-1018.
64. Zhou M, Huang C, Wysocki VH. Surface-induced dissociation of ion mobility-separated noncovalent complexes in a quadrupole/time-of-flight mass spectrometer. *Anal Chem*. 2012;84(14):6016-6023.
65. Zhou M, Dagan S, Wysocki VH. Protein subunits released by surface collisions of noncovalent complexes: nativelike compact structures revealed by ion mobility mass spectrometry. *Angew Chem Int Ed Engl*. 2012;51(18):4336-4339.
66. Haupt C, Hofmann T, Wittig S, Kostmann S, Politis A, Schmidt C. Combining chemical cross-linking and mass spectrometry of intact protein complexes to study the architecture of multi-subunit protein assemblies. *J Vis Exp: JoVE*. 2017;129:e56747.
67. Zhou M, Sandercock AM, Fraser CS, et al. Mass spectrometry reveals modularity and a complete subunit interaction map of the eukaryotic translation factor eIF3. *Proc Natl Acad Sci U S A*. 2008;105(47):18139-18144.
68. Rouillon C, Zhou M, Zhang J, et al. Structure of the CRISPR interference complex CSM reveals key similarities with cascade. *Mol Cell*. 2013;52(1):124-134.
69. van Duijn E, Barbu IM, Barendregt A, et al. Native tandem and ion mobility mass spectrometry highlight structural and modular similarities in clustered-regularly-interspaced shot-palindromic-repeats (CRISPR)-associated protein complexes from *Escherichia coli* and

Pseudomonas aeruginosa. *Mol Cell Proteomics: MCP*. 2012;11(11):1430-1441.
70. Rostom AA, Fucini P, Benjamin DR, et al. Detection and selective dissociation of intact ribosomes in a mass spectrometer. *Proc Natl Acad Sci*. 2000;97(10):5185-5190.
71. Hanson CL, Videler H, Santos C, Ballesta JP, Robinson CV. Mass spectrometry of ribosomes from *Saccharomyces cerevisiae*: implications for assembly of the stalk complex. *J Biol Chem*. 2004;279(41):42750-42757.
72. Ilag LL, Videler H, McKay AR, et al. Heptameric $(L12)_6$/L10 rather than canonical pentameric complexes are found by tandem MS of intact ribosomes from thermophilic bacteria. *Proc Natl Acad Sci U S A*. 2005;102(23):8192-8197.
73. Schmidt C, Beilsten-Edmands V, Robinson CV. Insights into eukaryotic translation initiation from mass spectrometry of macromolecular protein assemblies. *J Mol Biol*. 2016;428(2 Pt A):344-356.
74. Uetrecht C, Versluis C, Watts NR, et al. High-resolution mass spectrometry of viral assemblies: molecular composition and stability of dimorphic hepatitis B virus capsids. *Proc Natl Acad Sci U S A*. 2008;105(27):9216-9220.
75. Gordiyenko Y, Videler H, Zhou M, et al. Mass spectrometry defines the stoichiometry of ribosomal stalk complexes across the phylogenetic tree. *Mol Cell Proteomics: MCP*. 2010;9(8):1774-1783.
76. Gordiyenko Y, Deroo S, Zhou M, Videler H, Robinson CV. Acetylation of L12 increases interactions in the *Escherichia coli* ribosomal stalk complex. *J Mol Biol*. 2008;380(2):404-414.
77. Uetrecht C, Heck AJ. Modern biomolecular mass spectrometry and its role in studying virus structure, dynamics, and assembly. *Angew Chem Int Ed Engl*. 2011;50(36):8248-8262.
78. Fuerstenau SD, Benner WH, Thomas JJ, Brugidou C, Bothner B, Siuzdak G. Mass spectrometry of an intact virus. *Angew Chem Int Ed Engl*. 2001;40(3):541-544.
79. Uetrecht C, Watts NR, Stahl SJ, Wingfield PT, Steven AC, Heck AJ. Subunit exchange rates in Hepatitis B virus capsids are geometry- and temperature-dependent. *Phys Chem Chem Phys: PCCP*. 2010;12(41):13368-13371.
80. Pogan R, Schneider C, Reimer R, Hansman G, Uetrecht C. Norovirus-like VP1 particles exhibit isolate dependent stability profiles. *J Phys Condens Matter*. 2018;30(6):064006.
81. Shoemaker GK, van Duijn E, Crawford SE, et al. Norwalk virus assembly and stability monitored by mass spectrometry. *Mol Cell Proteomics: MCP*. 2010;9(8):1742-1751.
82. Wegener H, Mallagaray A, Schone T, et al. Human norovirus GII.4(MI001) P dimer binds fucosylated and sialylated carbohydrates. *Glycobiology*. 2017;27(11):1027-1037.
83. Mallagaray A, Creutznacher R, Dulfer J, et al. A post-translational modification of human Norovirus capsid protein attenuates glycan binding. *Nat Commun*. 2019;10(1):1320.
84. Snijder J, van de Waterbeemd M, Damoc E, et al. Defining the stoichiometry and cargo load of viral and bacterial nanoparticles by Orbitrap mass spectrometry. *J Am Chem Soc*. 2014;136(20):7295-7299.
85. van de Waterbeemd M, Snijder J, Tsvetkova IB, Dragnea BG, Cornelissen JJ, Heck AJ. Examining the heterogeneous genome content of multipartite viruses BMV and CCMV by native mass spectrometry. *J Am Soc Mass Spectrom*. 2016;27(6):1000-1009.
86. Tanford C, Reynolds JA. Characterization of membrane proteins in detergent solutions. *Biochim Biophys Acta*. 1976;457(2):133-170.
87. Rundlett KL, Armstrong DW. Mechanism of signal suppression by anionic surfactants in capillary electrophoresis-electrospray ionization mass spectrometry. *Anal Chem*. 1996;68(19):3493-3497.
88. Ilag LL, Ubarretxena-Belandia I, Tate CG, Robinson CV. Drug binding revealed by tandem mass spectrometry of a protein-micelle complex. *J Am Chem Soc*. 2004;126(44):14362-14363.
89. Barrera NP, Di Bartolo N, Booth PJ, Robinson CV. Micelles protect membrane complexes from solution to vacuum. *Science (New York, NY)*. 2008;321(5886):243-246.
90. Barrera NP, Isaacson SC, Zhou M, et al. Mass spectrometry of membrane transporters reveals subunit stoichiometry and interactions. *Nat Methods*. 2009;6(8):585-587.
91. Landreh M, Liko I, Uzdavinys P, et al. Controlling release, unfolding and dissociation of membrane protein complexes in the gas phase through collisional cooling. *Chem Commun (Camb)*. 2015;51(85):15582-15584.
92. Laganowsky A, Reading E, Hopper JT, Robinson CV. Mass spectrometry of intact membrane protein complexes. *Nat Protoc*. 2013;8(4):639-651.
93. Konijnenberg A, Yilmaz D, Ingolfsson HI, et al. Global structural changes of an ion channel during its gating are followed by ion mobility mass spectrometry. *Proc Natl Acad Sci U S A*. 2014;111(48):17170-17175.
94. Urner LH, Liko I, Yen HY, et al. Modular detergents tailor the purification and structural analysis of membrane proteins including G-protein coupled receptors. *Nat Commun*. 2020;11(1):564.
95. Esteban O, Bernal RA, Donohoe M, et al. Stoichiometry and localization of the stator subunits E and G in *Thermus thermophilus* H+-ATPase/synthase. *J Biol Chem*. 2008;283(5):2595-2603.
96. Stewart AG, Sobti M, Harvey RP, Stock D. Rotary ATPases: models, machine elements and technical specifications. *Bioarchitecture*. 2013;3(1):2-12.
97. Stewart AG, Laming EM, Sobti M, Stock D. Rotary ATPases—dynamic molecular machines. *Curr Opin Struct Biol*. 2014;25:40-48.
98. Mitchell P. Coupling of phosphorylation to electron and hydrogen transfer by a chemi-osmotic type of mechanism. *Nature*. 1961;191(4784):144-148.
99. Zhou M, Morgner N, Barrera NP, et al. Mass spectrometry of intact V-type ATPases reveals bound lipids and the effects of nucleotide binding. *Science (New York, NY)*. 2011;334(6054):380-385.
100. Abbas YM, Wu D, Bueler SA, Robinson CV, Rubinstein JL. Structure of V-ATPase from the mammalian brain. *Science (New York, NY)*. 2020;367(6483):1240-1246.
101. Schmidt C, Zhou M, Marriott H, Morgner N, Politis A, Robinson CV. Comparative cross-linking and mass spectrometry of an intact F-type ATPase suggest a role for phosphorylation. *Nat Commun*. 2013;4(1):1985.
102. Schmidt C, Beilsten-Edmands V, Mohammed S, Robinson CV. Acetylation and phosphorylation control both local and global stability of the chloroplast F1 ATP synthase. *Sci Rep*. 2017;7(1):44068.
103. Martens C, Stein RA, Masureel M, et al. Lipids modulate the conformational dynamics of a secondary multidrug transporter. *Nat Struct Mol Biol*. 2016;23(8):744-751.
104. Marcoux J, Wang SC, Politis A, et al. Mass spectrometry reveals synergistic effects of nucleotides, lipids, and drugs binding to a multidrug resistance efflux pump. *Proc Natl Acad Sci U S A*. 2013;110(24):9704-9709.
105. Fiorentino F, Bolla JR, Mehmood S, Robinson CV. The different effects of substrates and nucleotides on the complex formation of ABC transporters. *Structure (London, England: 1993)*. 2019;27(4):651-659. e3
106. Pyle E, Guo C, Hofmann T, et al. Protein-lipid interactions stabilize the oligomeric state of BOR1p from *Saccharomyces cerevisiae*. *Anal Chem*. 2019;91(20):13071-13079.
107. Pyle E, Kalli AC, Amillis S, et al. Structural lipids enable the formation of functional oligomers of the eukaryotic purine symporter UapA. *Cell Chem Biol*. 2018;25(7):840-848. e4
108. Gupta K, Donlan JAC, Hopper JTS, et al. The role of interfacial lipids in stabilizing membrane protein oligomers. *Nature*. 2017;541(7637):421-424.

109. Frick M, Schmidt C. Mass spectrometry—a versatile tool for characterising the lipid environment of membrane protein assemblies. *Chem Phys Lipids*. 2019;221:145-157.
110. Denisov IG, Sligar SG. Nanodiscs for structural and functional studies of membrane proteins. *Nat Struct Mol Biol*. 2016;23(6):481-486.
111. Bada Juarez JF, Harper AJ, Judge PJ, Tonge SR, Watts A. From polymer chemistry to structural biology: the development of SMA and related amphipathic polymers for membrane protein extraction and solubilisation. *Chem Phys Lipids*. 2019;221:167-175.
112. Hopper JT, Yu YT, Li D, et al. Detergent-free mass spectrometry of membrane protein complexes. *Nat Methods*. 2013;10(12):1206-1208.
113. Marty MT, Zhang H, Cui W, Blankenship RE, Gross ML, Sligar SG. Native mass spectrometry characterization of intact nanodisc lipoprotein complexes. *Anal Chem*. 2012;84(21):8957-8960.
114. Marty MT. A universal score for deconvolution of intact protein and native electrospray mass spectra. *Anal Chem*. 2020;92(6):4395-4401.
115. Reid DJ, Diesing JM, Miller MA, et al. MetaUniDec: high-throughput deconvolution of native mass spectra. *J Am Soc Mass Spectrom*. 2019;30(1):118-127.
116. Campuzano ID, Li H, Bagal D, et al. Native MS analysis of bacteriorhodopsin and an empty nanodisc by orthogonal acceleration time-of-flight, orbitrap and ion cyclotron resonance. *Anal Chem*. 2016;88(24):12427-12436.
117. Reid DJ, Keener JE, Wheeler AP, et al. Engineering nanodisc scaffold proteins for native mass spectrometry. *Anal Chem*. 2017;89(21):11189-11192.
118. Keener JE, Zambrano DE, Zhang G, et al. Chemical additives enable native mass spectrometry measurement of membrane protein oligomeric state within intact nanodiscs. *J Am Chem Soc*. 2019;141(2):1054-1061.
119. Henrich E, Sormann J, Eberhardt P, et al. From gene to function: cell-free electrophysiological and optical analysis of ion pumps in nanodiscs. *Biophys J*. 2017;113(6):1331-1341.
120. Henrich E, Peetz O, Hein C, et al. Analyzing native membrane protein assembly in nanodiscs by combined non-covalent mass spectrometry and synthetic biology. *Elife*. 2017;6:e20954.
121. Walker LR, Marzluff EM, Townsend JA, Resager WC, Marty MT. Native mass spectrometry of antimicrobial peptides in lipid nanodiscs elucidates complex assembly. *Anal Chem*. 2019;91(14):9284-9291.
122. Chorev DS, Baker LA, Wu D, et al. Protein assemblies ejected directly from native membranes yield complexes for mass spectrometry. *Science (New York, NY)*. 2018;362(6416):829-834.
123. Chorev DS, Tang H, Rouse SL, et al. The use of sonicated lipid vesicles for mass spectrometry of membrane protein complexes. *Nat Protoc*. 2020;15(5):1690-1706.
124. McDaniel EW, Mason EA. *Mobility and Diffusion of Ions in Gases*. United States: John Wiley and Sons, Inc; 1973.
125. Karasek FW. Plasma chromatography. *Anal Chem*. 1974;46(8):710A-720a.
126. Seo J, Hoffmann W, Warnke S, Bowers MT, Pagel K, von Helden G. Retention of native protein structures in the absence of solvent: a coupled ion mobility and spectroscopic study. *Angew Chem Int Ed*. 2016;55(45):14173-14176.
127. Ruotolo BT, Giles K, Campuzano I, Sandercock AM, Bateman RH, Robinson CV. Evidence for macromolecular protein rings in the absence of bulk water. *Science (New York, NY)*. 2005;310(5754):1658-1661.
128. Buryakov IA, Krylov EV, Nazarov EG, Rasulev UK. A new method of separation of multi-atomic ions by mobility at atmospheric pressure using a high-frequency amplitude-asymmetric strong electric field. *Int J Mass Spectrom Ion Process*. 1993;128(3):143-148.
129. Kolakowski BM, Mester Z. Review of applications of high-field asymmetric waveform ion mobility spectrometry (FAIMS) and differential mobility spectrometry (DMS). *Analyst*. 2007;132(9):842-864.
130. Jarrold MF. Peptides and proteins in the vapor phase. *Annu Rev Phys Chem*. 2000;51(1):179-207.
131. Mason EA, Schamp HW. Mobility of gaseous Ions in weak electric fields. *Ann Phys Rehabil Med*. 1958;4(3):233-270.
132. Giles K, Pringle SD, Worthington KR, Little D, Wildgoose JL, Bateman RH. Applications of a travelling wave-based radio-frequency-only stacked ring ion guide. *Rapid Commun Mass Spectrom*. 2004;18(20):2401-2414.
133. Giles K, Ujma J, Wildgoose J, et al. A cyclic ion mobility-mass spectrometry system. *Anal Chem*. 2019;91(13):8564-8573.
134. Eldrid C, Ujma J, Kalfas S, et al. Gas phase stability of protein ions in a cyclic ion mobility spectrometry traveling wave device. *Anal Chem*. 2019;91(12):7554-7561.
135. Kune C, Far J, De Pauw E. Accurate drift time determination by traveling wave ion mobility spectrometry: the concept of the diffusion calibration. *Anal Chem*. 2016;88(23):11639-11646.
136. Bush MF, Hall Z, Giles K, Hoyes J, Robinson CV, Ruotolo BT. Collision cross sections of proteins and their complexes: a calibration framework and database for gas-phase structural biology. *Anal Chem*. 2010;82(22):9557-9565.
137. Ruotolo BT, Benesch JL, Sandercock AM, Hyung SJ, Robinson CV. Ion mobility-mass spectrometry analysis of large protein complexes. *Nat Protoc*. 2008;3(7):1139-1152.
138. Sivalingam GN, Yan J, Sahota H, Thalassinos K. Amphitrite: a program for processing travelling wave ion mobility mass spectrometry data. *Int J Mass Spectrom*. 2013;345-347:54-62.
139. Allison TM, Reading E, Liko I, Baldwin AJ, Laganowsky A, Robinson CV. Quantifying the stabilizing effects of protein-ligand interactions in the gas phase. *Nat Commun*. 2015;6(1):8551.
140. Migas LG, France AP, Bellina B, Barran PE. ORIGAMI: a software suite for activated ion mobility mass spectrometry (aIM-MS) applied to multimeric protein assemblies. *Int J Mass Spectrom*. 2018;427:20-28.
141. Sivalingam GN, Cryar A, Williams MA, Gooptu B, Thalassinos K. Deconvolution of ion mobility mass spectrometry arrival time distributions using a genetic algorithm approach: application to α1-antitrypsin peptide binding. *Int J Mass Spectrom*. 2018;426:29-37.
142. Fernandez-Lima FA, Kaplan DA, Park MA. Note: Integration of trapped ion mobility spectrometry with mass spectrometry. *Rev Sci Instrum*. 2011;82(12):126106.
143. Liu FC, Ridgeway ME, Park MA, Bleiholder C. Tandem trapped ion mobility spectrometry. *Analyst*. 2018;143(10):2249-2258.
144. Silveira JA, Michelmann K, Ridgeway ME, Park MA. Fundamentals of trapped ion mobility spectrometry part II: fluid dynamics. *J Am Soc Mass Spectrom*. 2016;27(4):585-595.
145. Michelmann K, Silveira JA, Ridgeway ME, Park MA. Fundamentals of trapped ion mobility spectrometry. *J Am Soc Mass Spectrom*. 2015;26(1):14-24.
146. Hernandez DR, Debord JD, Ridgeway ME, Kaplan DA, Park MA, Fernandez-Lima F. Ion dynamics in a trapped ion mobility spectrometer. *Analyst*. 2014;139(8):1913-1921.
147. Chai M, Young MN, Liu FC, Bleiholder C. A Transferable, sample-independent calibration procedure for trapped ion mobility spectrometry (TIMS). *Anal Chem*. 2018;90(15):9040-9047.
148. Naylor CN, Reinecke T, Ridgeway ME, Park MA, Clowers BH. Validation of calibration parameters for trapped ion mobility spectrometry. *J Am Soc Mass Spectrom*. 2019;30(10):2152-2162.
149. Politis A, Park AY, Hall Z, Ruotolo BT, Robinson CV. Integrative modelling coupled with ion mobility mass spectrometry reveals structural features of the clamp loader in complex with single-stranded DNA binding protein. *J Mol Biol*. 2013;425(23):4790-4801.

150. Hall Z, Politis A, Robinson CV. Structural modeling of heteromeric protein complexes from disassembly pathways and ion mobility-mass spectrometry. *Structure (London, England: 1993)*. 2012;20(9):1596-1609.
151. Mack E. Average cross-sectional areas of molecules by gaseous diffusion methods. *J Am Chem Soc*. 1925;47(10):2468-2482.
152. Mesleh MF, Hunter JM, Shvartsburg AA, Schatz GC, Jarrold MF. Structural information from ion mobility measurements: effects of the long-range potential. *J Phys Chem*. 1996;100(40):16082-16086.
153. Paizs B. A divide-and-conquer approach to compute collision cross sections in the projection approximation method. *Int J Mass Spectrom*. 2015;378:360-363.
154. Marklund EG, Degiacomi MT, Robinson CV, Baldwin AJ, Benesch JL. Collision cross sections for structural proteomics. *Structure (London, England: 1993)*. 2015;23(4):791-799.
155. Bleiholder C, Wyttenbach T, Bowers MT. A novel projection approximation algorithm for the fast and accurate computation of molecular collision cross sections (I). Method. *Int J Mass Spectrom*. 2011;308(1):1-10.
156. Anderson SE, Bleiholder C, Brocker ER, Stang PJ, Bowers MT. A novel projection approximation algorithm for the fast and accurate computation of molecular collision cross sections (III): application to supramolecular coordination-driven assemblies with complex shapes. *Int J Mass Spectrom*. 2012;330-332:78-84.
157. Bleiholder C, Contreras S, Bowers MT. A novel projection approximation algorithm for the fast and accurate computation of molecular collision cross sections (IV). Application to Polypeptides. *Int J Mass Spectrom*. 2013;354-355:275-280.
158. Bleiholder C, Contreras S, Do TD, Bowers MT. A novel projection approximation algorithm for the fast and accurate computation of molecular collision cross sections (II). Model parameterization and definition of empirical shape factors for proteins. *Int J Mass Spectrom*. 2013;345-347:89-96.
159. Bleiholder C. A local collision probability approximation for predicting momentum transfer cross sections. *Analyst*. 2015;140(20):6804-6813.
160. Shvartsburg AA, Jarrold MF. An exact hard-spheres scattering model for the mobilities of polyatomic ions. *Chem Phys Lett*. 1996;261(1):86-91.
161. Lee JW, Davidson KL, Bush MF, Kim HI. Collision cross sections and ion structures: development of a general calculation method via high-quality ion mobility measurements and theoretical modeling. *Analyst*. 2017;142(22):4289-4298.
162. Alexeev Y, Fedorov DG, Shvartsburg AA. Effective ion mobility calculations for macromolecules by scattering on electron clouds. *Chem A Eur J*. 2014;118(34):6763-6772.
163. Laszlo KJ, Bush MF. Effects of charge state, charge distribution, and structure on the ion mobility of protein ions in helium gas: results from trajectory method calculations. *Chem A Eur J*. 2017;121(40):7768-7777.
164. Ewing SA, Donor MT, Wilson JW, Prell JS. Collidoscope: an improved tool for computing collisional cross-sections with the trajectory method. *J Am Soc Mass Spectrom*. 2017;28(4):587-596.
165. Lanucara F, Holman SW, Gray CJ, Eyers CE. The power of ion obility-mass spectrometry for structural characterization and the study of conformational dynamics. *Nat Chem*. 2014;6(4):281-294.
166. Wyttenbach T, Pierson NA, Clemmer DE, Bowers MT. Ion mobility analysis of molecular dynamics. *Annu Rev Phys Chem*. 2014;65(1):175-196.
167. Goth M, Pagel K. Ion mobility-mass spectrometry as a tool to investigate protein-ligand interactions. *Anal Bioanal Chem*. 2017;409(18):4305-4310.
168. Eschweiler JD, Rabuck-Gibbons JN, Tian Y, Ruotolo BT. CIUSuite: a quantitative analysis package for collision induced unfolding measurements of gas-phase protein ions. *Anal Chem*. 2015;87(22):11516-11522.
169. Polasky DA, Dixit SM, Fantin SM, Ruotolo BT. CIUSuite 2: next-generation software for the analysis of gas-phase protein unfolding data. *Anal Chem*. 2019;91(4):3147-3155.
170. Hopper JT, Oldham NJ. Collision induced unfolding of protein ions in the gas phase studied by ion mobility-mass spectrometry: the effect of ligand binding on conformational stability. *J Am Soc Mass Spectrom*. 2009;20(10):1851-1858.
171. Hyung SJ, Robinson CV, Ruotolo BT. Gas-phase unfolding and disassembly reveals stability differences in ligand-bound multiprotein complexes. *Chem Biol*. 2009;16(4):382-390.
172. Beveridge R, Migas LG, Payne KAP, Scrutton NS, Leys D, Barran PE. Mass spectrometry locates local and allosteric conformational changes that occur on cofactor binding. *Nat Commun*. 2016;7(1):12163.
173. Laganowsky A, Reading E, Allison TM, et al. Membrane proteins bind lipids selectively to modulate their structure and function. *Nature*. 2014;510(7503):172-175.
174. Yefremova Y, Opuni KFM, Danquah BD, Thiesen HJ, Glocker MO. Intact transition epitope mapping (ITEM). *J Am Soc Mass Spectrom*. 2017;28(8):1612-1622.
175. Danquah BD, Yefremova Y, Opuni KFM, Rower C, Koy C, Glocker MO. Intact transition epitope mapping–thermodynamic weak-force order (ITEM-TWO). *J Proteomics*. 2020;212:103572.
176. Danquah BD, Rower C, Opuni KFM, et al. Intact transition epitope mapping–targeted high-energy rupture of extracted epitopes (ITEM-THREE). *Mol Cell Proteomics: MCP*. 2019;18(8):1543-1555.
177. Hoffmann W, Folmert K, Moschner J, et al. NFGAIL amyloid oligomers: the onset of beta-sheet formation and the mechanism for fibril formation. *J Am Chem Soc*. 2018;140(1):244-249.
178. Seo J, Hoffmann W, Warnke S, et al. An infrared spectroscopy approach to follow beta-sheet formation in peptide amyloid assemblies. *Nat Chem*. 2017;9(1):39-44.
179. Cole H, Porrini M, Morris R, et al. Early stages of insulin fibrillogenesis examined with ion mobility mass spectrometry and molecular modelling. *Analyst*. 2015;140(20):7000-7011.
180. Bleiholder C, Dupuis NF, Wyttenbach T, Bowers MT. Ion mobility-mass spectrometry reveals a conformational conversion from random assembly to beta-sheet in amyloid fibril formation. *Nat Chem*. 2011;3(2):172-177.
181. Rose RJ, Damoc E, Denisov E, Makarov A, Heck AJ. High-sensitivity Orbitrap mass analysis of intact macromolecular assemblies. *Nat Methods*. 2012;9(11):1084-1086.
182. Gault J, Donlan JA, Liko I, et al. High-resolution mass spectrometry of small molecules bound to membrane proteins. *Nat Methods*. 2016;13(4):333-336.
183. Wu D, Li J, Struwe WB, Robinson CV. Probing N-glycoprotein microheterogeneity by lectin affinity purification-mass spectrometry analysis. *Chem Sci*. 2019;10(19):5146-5155.
184. van de Waterbeemd M, Fort KL, Boll D, et al. High-fidelity mass analysis unveils heterogeneity in intact ribosomal particles. *Nat Methods*. 2017;14(3):283-286.
185. Belov ME, Damoc E, Denisov E, et al. From protein complexes to subunit backbone fragments: a multi-stage approach to native mass spectrometry. *Anal Chem*. 2013;85(23):11163-11173.
186. Ben-Nissan G, Belov ME, Morgenstern D, et al. Triple-stage mass spectrometry unravels the heterogeneity of an endogenous protein complex. *Anal Chem*. 2017;89(8):4708-4715.
187. Gault J, Liko I, Landreh M, et al. Combining native and 'omics' mass spectrometry to identify endogenous ligands bound to membrane proteins. *Nat Methods*. 2020;17(5):505-508.
188. Bolla JR, Corey RA, Sahin C, et al. A mass-spectrometry-based approach to distinguish annular and specific lipid binding to membrane proteins. *Angew Chem Int Ed Engl*. 2020;59(9):3523-3528.

189. Yen HY, Hoi KK, Liko I, et al. PtdIns(4,5)P_2 stabilizes active states of GPCRs and enhances selectivity of G-protein coupling. *Nature*. 2018;559(7714):423-427.
190. Leney AC, Rafie K, van Aalten DMF, Heck AJR. Direct monitoring of protein O-GlcNAcylation by high-resolution native mass spectrometry. *ACS Chem Biol*. 2017;12(8):2078-2084.
191. Rodenburg RNP, Snijder J, van de Waterbeemd M, et al. Stochastic palmitoylation of accessible cysteines in membrane proteins revealed by native mass spectrometry. *Nat Commun*. 2017;8(1):1280.
192. Poltash ML, McCabe JW, Shirzadeh M, Laganowsky A, Russell DH. Native IM-Orbitrap MS: resolving what was hidden. *Trends Anal Chem: TRAC*. 2020;124:115533.

How to cite this article: Barth M, Schmidt C. Native mass spectrometry—A valuable tool in structural biology. *J Mass Spectrom*. 2020;55:e4578. https://doi.org/10.1002/jms.4578